

Article

Spatial Optimization of Land Use Pattern toward Carbon Mitigation Targets—A Study in Guangzhou

Shouyi Ding^{1,2,3}, Shumi Liu⁴, Mingxin Chang⁴, Hanwei Lin^{1,2,3}, Tianyu Lv², Yujing Zhang^{1,2,3} and Chen Zeng^{4,*}

- ¹ Guangzhou Urban Planning & Design Survey Research Institute, Guangzhou 510060, China; dingshouyi@gzpi.com.cn (S.D.); linhanwei@gzpi.com.cn (H.L.); zhangyujing@gzpi.com.cn (Y.Z.)
- ² Guangzhou Collaborative Innovation Center of Natural Resources Planning and Marine Technology, Guangzhou 510060, China; tianyulv97@webmail.hzau.edu.cn
- ³ Guangdong Enterprise Key Laboratory for Urban Sensing Monitoring and Early Warning, Guangzhou 510060, China
- ⁴ Department of Land Management, Huazhong Agricultural University, Wuhan 430070, China; lsm_6@webmail.hzau.edu.cn (S.L.); changmx@webmail.hzau.edu.cn (M.C.)
- * Correspondence: zengchen@igsnr.ac.cn; Tel.: +86-132-9668-3817

Abstract: Global climate change is one of the major challenges facing the world, and the spatial optimization of land use patterns has been regarded as critical in realizing carbon mitigation. In this study, the linear programming model and the Markov Chain model are integrated in different scenarios to optimize land use structure for low-carbon development. The land use pattern is then simulated through the adjusted convolutional neural network and cellular automata model, taking Guangzhou City as the case study area. The results reveal that construction land with high economic efficiency will increase its area, and the remaining types will experience slight changes, in 2035 in the natural development scenario and the economic priority scenario. Ecological land such as forest land, grassland, and water is partly occupied by construction land in the urban–rural fringe areas. The total carbon emissions decrease by 2.32% and 1.57% in these two scenarios. In the low-carbon-oriented scenario, the expansion of construction land is restricted, and the forest land and grassland undergo great expansion. The total carbon emission decreases by 18.95%—a figure much larger than that in the natural development scenario and the economic priority scenario. Our paper embeds the needs and constraints in land spatial planning into the spatial optimization of the land use pattern, which provides valuable references for low-carbon city development in the future.

Keywords: carbon emission; land use; spatial optimization; scenario simulation; Guangzhou City



Citation: Ding, S.; Liu, S.; Chang, M.; Lin, H.; Lv, T.; Zhang, Y.; Zeng, C. Spatial Optimization of Land Use Pattern toward Carbon Mitigation Targets—A Study in Guangzhou. *Land* **2023**, *12*, 1903. <https://doi.org/10.3390/land12101903>

Academic Editors: Helen Bao, Hossein Azadi and Jie Liu

Received: 6 September 2023
Revised: 2 October 2023
Accepted: 5 October 2023
Published: 10 October 2023



Copyright: © 2023 by the authors. Licensee MDPI, Basel, Switzerland. This article is an open access article distributed under the terms and conditions of the Creative Commons Attribution (CC BY) license (<https://creativecommons.org/licenses/by/4.0/>).

1. Introduction

Global warming has a profound influence on human survival and development, and is one of the major challenges facing countries worldwide [1]. Land use affects the carbon cycle of terrestrial ecosystems by changing the natural surface cover and the intensity of human activities, which is one of the main factors of the greenhouse effect. Changes in land use and land management contribute around 14% of the total global anthropogenic CO₂ emissions [2]. As a major agglomeration of human socioeconomic activities, construction land is the largest source of greenhouse gas emissions. The expansion of construction land in the urbanization continues to encroach on carbon sink land categories, leading to a continuous decline in the overall regional capacity for carbon storage and sequestration by vegetation [3]. The spatial optimization of land use facilitates improving the carbon emission efficiency of land use, enhances the “carbon sequestration capacity” of the land system, and refixes 60–70% of the depleted carbon [4]. The proper planning and management of construction land based on scientific logic is becoming especially important in relation to preventing the increase in greenhouse gas emissions.

In the context of the “dual carbon” strategy in China, there have been substantial transformations in socioeconomic development, as well as human activities. Land use patterns have thus also been greatly influenced by focusing on controlling the scale of urban construction land, with a high intensity of land emission, and conserving ecological land with carbon sink functions, such as forest and grassland [5]. Construction land is primarily regarded as a carbon source, whereas ecological land such as forest and water serves as a carbon sink. Researchers are concerned with the topics of urbanization and the expansion of construction land, built-up land intensity, and green land development [6]. Scholars have also discussed the feasibility of China’s carbon neutrality in 2060 and the distribution of carbon sinks in the scenarios of different land use patterns, which demonstrates that the expansion of construction land should be limited in the future [7]. Moreover, one dilemma is that China’s current environmental conditions and ecological environment can hardly allow the coexistence of high construction land development intensity and high carbon emissions [8]. Hence, controlling the scale of construction land and improving the degree of intensive conservation of construction land are powerful measures to reduce carbon emissions. Forest land and grassland are important carbon sinks. Scholars have shown that the conservation and restoration of forest and grassland waters and increasing the proportion of forest and grassland can effectively enhance the carbon sink of urban ecosystems [9,10]. Pragmatically, China’s rapid urbanization and industrialization have led to dramatic changes in land use in the past several decades, and the uncontrolled expansion of urban construction land has led to the intensification of spatial conflicts in the existing “three zones and three lines”, the imbalance between carbon source and carbon sink scale, and the rising carbon emissions [11]. Land spatial planning is a basic, binding mode of planning to guide land use, regional development, urban and rural construction, and ecological protection, and it is a blueprint for the protection, utilization, and restoration of land spatial resources [12]. Basing land spatial planning on the carbon reduction target can promote the synergy between the development and utilization of land and the low-carbon target, regulate the total amount and boundaries of production, living and ecological space, constrain the scale of carbon sources in urban space, and consolidate the scale of carbon sinks in ecological and agricultural space [13]. Carbon mitigation-related research with respect to land use change and land use planning will help us to explore carbon emission reduction pathways in cities, which is important for building a low-carbon land spatial pattern and realizing a balance between socioeconomic development and eco-environmental protection [14].

With the advent and popularity of geospatial data and intelligent models, the research on carbon emissions combined with land use change continues to deepen. In recent years, land use carbon emission accounting [15,16], the driving mechanism of land use-related carbon source and sink changes [17], and low-carbon land use optimization [18] have become mainstream. The land use carbon accounting method is closely related to the datasets available at various times. In the early days, the carbon emissions of land use were calculated via the sample plot inventory method or the system dynamic model [19,20]. Based on national forest resource inventory data, scholars in China established biomass conversion factors to estimate the carbon storage of major ground plants in China in the past 20 years [21]. Later, with the development of remote sensing technologies, the interpreted land use data and other geospatial information were utilized to measure carbon emissions [22,23]. At present, studies are based on the IPCC’s National Greenhouse Gas Emission Inventory, which integrates different data sources [24,25]. These datasets and generated data products on carbon emissions in relation to land use provide information essential to comprehending the relationship between land use and carbon emissions in different cities and regions [15]. In terms of optimization models, scholars have conducted a series of studies on the optimization of the land use quantity structure and spatial layout by setting different development paths and development goals [26,27]. The optimization of land use can change the carbon source/sink pattern, thereby guiding the low-carbon transformation and sustainable development of the regional social economy [28]. In ad-

dition to the traditional optimization of the quantities of different land use types using programming models for balancing ecological and socioeconomic benefits, spatial optimization models such as the cellular automata (CA) model have been widely applied for their applicability in unearthing the optimal land use pattern for climate change mitigation and adaptation [29]. For example, Huang et al. analyzed the carbon emissions of Jinhua City in 2030 under different scenarios based on the linear programming model and the CA model, and proposed a land use structure and layout with the least carbon emissions [14]. Li et al. set differentiated carbon emission and economic and ecological benefit constraint objectives based on the linear programming model and conducted land spatial zoning optimization simulations through the PLUS model [29]. These models and empirical studies have set the tone in how the optimization of future land spatial pattern can be realized with the consideration of carbon mitigation goals. Although scholars have conducted substantial research on land use and carbon emission, the context of future land use or urban planning has not been fully integrated, resulting in the insufficient feasibility and practicability of research. Furthermore, future land use simulation (FLUS) [30], PLUS [31], CLUE-S [32], and other intelligent models developed based on CA have been widely applied in the extant research, yet ignorance with regard to human development and socioeconomic factors still exists, which constrains model accuracy.

To address the gaps in the lack of the integration of local land use and urban planning, as well as local socioeconomic development, in the prediction, simulation and optimization of land use patterns, this study applies linear programming and the adjusted cellular automata model with the consideration of local conditions, taking Guangzhou city as an example. It attempts to establish a research framework to link future land spatial plans with carbon mitigations to promote low-carbon development in cities.

2. Materials and Methods

2.1. Study Area and Data Description

Guangzhou is in the south of mainland China, in the south-central part of Guangdong Province. Guangzhou is the industrial, economic heart of Guangdong Province, including 11 districts (Figure 1). This city had 18.73 million permanent residents and an urbanization rate of 86.48% in 2022. With rapid development, the area of construction land increased by 45.72% in Guangzhou, while the areas of forest and grass decreased by 2.65% and 75.60%, respectively.

Since the implementation of policies focused on energy restructuring, industrial transformation and upgrading, and traffic management in 2005, the carbon emissions of Guangzhou decreased by 20.73%. However, the population explosion and unprecedented urbanization have placed heavy pressure on Carbon Neutral Targets, and a low-carbon land use pattern still needs to be explored to tackle the serious challenges.

This study uses a geospatial dataset in the forms of raster and vector, as well as statistical dataset and generated dataset products with multiple data sources. Land use in Guangzhou is classified into six types: cultivated land, forest, grassland, water, construction land, and unused land. The main impact factor data used in the paper include China's high-spatial-resolution emission grid data (CHRED) provided by the China Cities Greenhouse Gas Work Platform, land use data released by the Geographic State Monitoring Cloud Platform, and physical geographic and socioeconomic data from multiple time periods, as shown in Table 1.

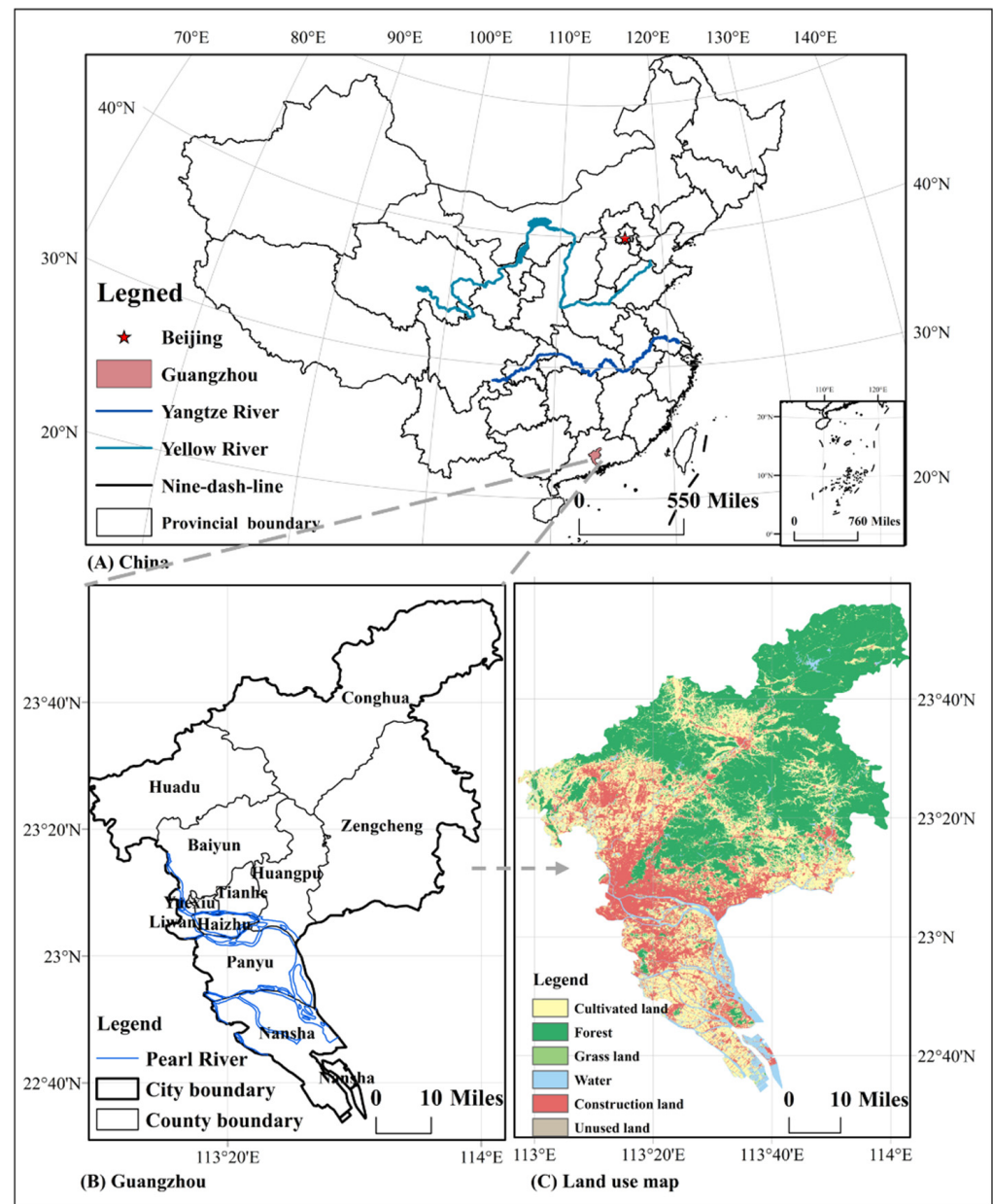


Figure 1. Location and administrative divisions of Guangzhou.

2.2. Methods

Figure 2 shows the land use data and the natural and socioeconomic driver force data of Guangzhou that were used in this paper to predict and simulate future land use patterns, including two subsections: (1) Land use demand prediction. Three scenarios were set based on urban development and future socioeconomic planning. The land use structure in 2035 of the natural development scenario was calculated based on the Markov Chain model. Land use structures oriented toward low-carbon economic priorities were projected through the Gray Predicting model and the Linear Programming model. (2) Land use spatial layout simulation. The driver forces of land use transformation from physical geography datasets and socioeconomic datasets were selected, and the probability layers of various land use types were predicted by the convolution neural network (CNN) and random forest (RF) classifier, which were combined with a restricted layer as the input of CA to simulate the future land use spatial layout.

Table 1. Overview of dataset.

Name	Time Range	Format	Source	Description
Land use	2000–2020	Raster (30 m × 30 m)	http://www.dsac.cn/DataProduct/Index/200804 (accessed on 15 June 2023)	Land use types, areas, and spatial pattern
DEM (Digital Elevation Model)	2020	Raster (1 km × 1 km)	http://www.dsac.cn/DataProduct/Index/200804 (accessed on 20 June 2023)	Spatial raster dataset describing the elevation and slope
Slope	2020	Raster (1 km × 1 km)	Calculated by DEM HWSD	Spatial soil dataset describing the soil properties of density, topsoil organic carbon, clay fraction, sand fraction and texture
Soil data	2009	Raster (1 km × 1 km)	(http://www.fao.org/soils-portal/soil-survey/soil-maps-and-databases/harmonized-world-soil-database-v12/en/ (accessed on 20 June 2023)) Resource and Environment Science and Data Center (https://www.resdc.cn/Default.aspx (accessed on 20 June 2023))	Dataset describing the spatial distribution of the rivers
River network	2005	Shapefile	WorldPop (https://www.worldpop.org/ (accessed on 20 June 2023))	Spatial data dataset describing the spatial distribution of population
Population density	2020	Raster (1 km × 1 km)	http://59.175.109.173:8888/index.html (accessed on 20 June 2023)	Dataset describing the spatial distributions of infrastructure and public facilities such as school, hospital, park, et al.
Nighttime-light Dataset	2020	Raster (1 km × 1 km)	AutoNavi Open Platform	Statistical dataset describing the socioeconomic levels in Guangzhou
Subway station points	2020	Shapefile	Guangzhou Statistical Yearbook (2000–2020)	Statistical dataset describing the socioeconomic levels in Guangzhou
Social services (School, hospital, park, hotel, bank, and supermarket)	2020	Shapefile		Dataset describing CO ₂ emissions in the Chinese cities
GDP	2000–2020	Statistical data		
Resident population	2000–2020	Statistical data		
Added value of agriculture, forestry, animal husbandry, and by-fishery industries	2000–2020	Statistical data		
CO ₂ emissions dataset	2005, 2010, 2015, and 2020	Dataset	http://www.cityghg.com/ (accessed on 20 June 2023)	

2.2.1. Relationship between Land Use and Carbon Emissions

The heterogeneity of the physicochemical properties and functions of different land types leads to dissimilarities in the relationship between land use types and carbon emissions. Therefore, different coefficients should be used to calculate the carbon emissions from diverse land use types, which have been widely used by scholars. In this paper, the previous parameters were obtained from the studies showed in Table 2 and adjusted according to the actual situation of Guangzhou. The equation is as follows:

$$C_i = K_i \times S_i \quad (1)$$

where C_i denotes the carbon emission of land type i , K_i denotes the carbon emission coefficient of land type i , and S_i denotes the area of land type i .

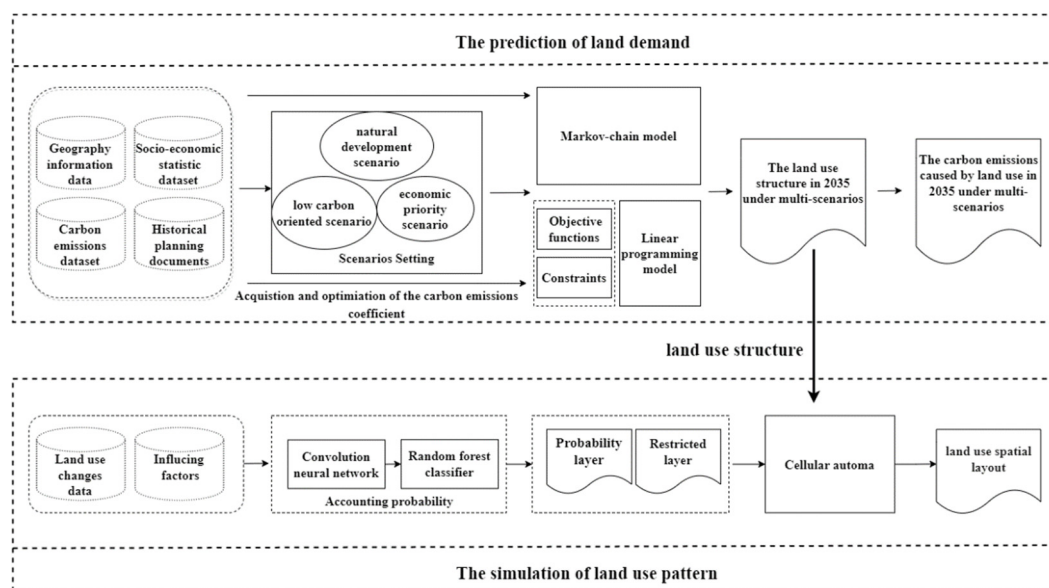


Figure 2. Technical route.

- Carbon emission coefficient of cultivated land. Cultivated land is a carbon sink and a carbon source, which can be considered in two ways: (1) With the utilization of fertilizers and farm machinery, cultivated land can be considered a carbon source. (2) Crops can absorb and store carbon during growth. However, most studies treated cultivated land as a carbon source [33]. In this paper, cultivated land is also considered a carbon source. Due to the high density of human activities on cultivated land, the carbon emission coefficient is not stable and needs to be determined by linear regression based on historical data [34]. The carbon emission factor of cultivated land in Guangzhou in 2035 is calculated as 181.735 t/km^2 .
- Carbon emission coefficient of forest and grass land. These two land use types have a carbon sink capacity that is affected by a variety of factors, such as climate, vegetation, and the chemical and biological properties of the soil, which are generally stable and do not undergo substantial changes in the short term [35,36]. Thus, the carbon emission coefficients of forest and grass land obtained from the existing studies are -57.8 and -2.1 t/km^2 , respectively [37].
- Carbon emission coefficient of water. According to the previous studies, water areas are usually considered a carbon sink [35]. The carbon coefficient of water areas in this paper is -25.2 t/km^2 [37].
- Carbon emission coefficient of construction land. Carbon emissions from construction land are closely related with the high intensity of human activities. With the expansion of construction land, the encroachment of ecological space and growth in energy consumption sharply increase the carbon emissions [38]. The carbon emissions from construction land can be accounted by a mature methodological system and have been proven to be in a constant state of change by existing studies [34,39,40]. Thus, the time series pattern of carbon emissions from construction land needs to be explored based on historical carbon emissions to determine future carbon emissions. Based on this, the CHRED was used to match the spatial relationship between industries and land use type, account for the carbon emission coefficient of cultivated land and construction land from 2005 to 2020 to explore the carbon emission coefficient change pattern, and project the carbon emission coefficient in 2035, which can be used to determine the carbon emissions from construction land in 2035 using the Gray Prediction model. The carbon emission coefficient is set as $27,993.95 \text{ t/km}^2$ in this paper.
- Carbon emission of unused land. Unused land consists of wasteland and bare ground. The capacities for carbon emissions and carbon sink of unused land are

weak. According to existing studies, the carbon emission coefficient of unused land is -0.5 t/km^2 [37].

Table 2. Definition of carbon emissions and sinks in different land use types and references for site studies.

Land Use Type	Carbon Source/Sink	Site Experiment
Cultivated land	Carbon source	Sichuan Province [33]; Guangdong Province [41]
Forest	Carbon sink	
Grassland	Carbon sink	Mainland China [37,42]
Water	Carbon sink	
Unused land	Carbon sink	
Construction land	Carbon source	Pearl River Delta [39]

2.2.2. Land Use Demand Prediction in Multiple Scenarios

The areas of various land types of Guangzhou under different scenarios in 2035 can be calculated based on the Markov Chain model and the Linear Programming model. The land use area transfer matrix and transfer probability can be discovered by the Markov Chain model to determine the transformation trend between different land use types [43]. The Linear Programming model, which is an important model for studies about the optimization of land use structure, is a basic mathematical model for examining the geography and the development of regional economics. Decision variables, objective functions, and constraints are included in the Linear Programming model, which can be shown in the following formulas:

$$F(x) = \min(\max) \sum_{j=1}^n K_j \times x_j \quad (2)$$

$$s.t. = \sum_{j=1}^n a_{ij}x_j = (\geq, \leq) b_j, (i = 1, 2, 3 \dots, m) \quad (3)$$

where $F(x)$ denotes total carbon emissions, x_j denotes the decision variable j ($j = 1, 2, 3, \dots, m$), $x_j \geq 0$, and K_j denotes optimized carbon emission coefficients or economic efficiency coefficients; in the constraints *s.t.*, a_{ij} is the coefficient corresponding to the j -th variable in the i -th constraint, and b_j is the constraint value.

Three scenarios in 2035 were set based on the transformation of land use types in Guangzhou from 2005 to 2020, in “Outline of the Fourteenth Five-Year Plan for the National Economic and Social Development of Guangzhou Municipality and the Vision 2035” and “Guangzhou City Territorial Spatial Master Plan (2021–2035)”:

- Natural development scenario. This scenario does not consider the other factors’ effects of land use type transformation. The natural development scenario is the control group for other scenarios—it just obeys the historical pattern of land use change from 2005 to 2020. The land use demands under the natural development scenario in 2035 are predicted by the Markov Chain model [44];
- Low carbon-oriented scenario. This scenario concentrates on the high carbon sink and low carbon emissions from land use sectors. Under this scenario, the total carbon emissions should be the lowest among the three scenarios [45], the carbon reduction benefits of high-carbon sink land use types should be utilized fully, the ecological land protection should be enhanced, and the rough expansion of high-carbon emission land should be seriously limited. The areas of land use types, such as forest and grassland, that can absorb carbon should not be less than those in 2020;
- Economic priority scenario. The goal of this scenario is to maximize economic rewards. Therefore, construction land maximizes expansion within the constraints of food security and ecological benefits [46].

Based on the current land use classification, six land types, namely, cultivated land (X_1), forest (X_2), grassland (X_3), water (X_4), construction land (X_5), and unused land (X_6),

were selected as the decision variables. The objective functions were set through the optimized carbon emission coefficients and economic efficiency coefficients. Considering food demand and ecological efficiency, the detail constraints of various land types were set, as shown in Table 3. The constraints for each land use type were set as follows: (1) Cultivated land. According to the “Guangzhou City Territorial Spatial Master Plan (2021–2035)”, the area of basic permanent farmland and the holdings of cultivated land in 2035 should not be less than those in 2020. (2) Water. According to the “Guangzhou Water Management Regulations”, “Measures for the Administration of Guangzhou Municipal Construction Projects Occupying Waters”, and other documents on the strict management of water areas, the areas of water set in this paper were not changed. (3) Grassland and unused land. The areas of these two land use types were set based on their original spatial distribution and change rates. (4) Construction land. According to the urban development boundary set in “Guangzhou City Territorial Spatial Master Plan (2021–2035)” and the requirements of economic development set in “Outline of the Fourteenth Five-Year Plan for the National Economic and Social Development of Guangzhou Municipality and the Vision 2035”, the area of construction in 2035 was set as less than the urban development boundary and more than that in 2020. (5) Forest. According to the red line for ecological protection set in “Guangzhou City Territorial Spatial Master Plan (2021–2035)” and the rules to protect forests in “Regulations on the Protection and Management of Forests in Guangdong Province”, the area of forest should not less than the area required by the red line for ecological protection. To satisfy the requirements of the low-carbon-oriented scenario and the economic scenario, the rate of forest cover should not be less than 0.416 for the former, and the decrease rate of forest area should less than it in past decade for the latter. In addition, the economic development goals constraint and development intensity constraint were set based on “Guangzhou City Territorial Spatial Master Plan (2021–2035)” and “Outline of the Fourteenth Five-Year Plan for the National Economic and Social Development of Guangzhou Municipality and the Vision 2035”.

Table 3. Constraint setting and reference.

Factors	Constraint Expressions	Reference
Total area	$\sum X_i = TA$	“Guangzhou City Territorial Spatial Master Plan (2018–2035)” (http://ghzyj.gz.gov.cn/zwgk/ztzl/gtkjgh/gzxx/content/post_6484475.html (accessed on 22 June 2023))
Cultivated Land area	$X1 \geq CLQ$ $X1 \geq BPCLA$	
Forest area	$X2 \geq TA * 0.416$ (LCS)	1. “Guangzhou City Territorial Spatial Master Plan (2018–2035)” (http://ghzyj.gz.gov.cn/zwgk/ztzl/gtkjgh/gzxx/content/post_6484475.html (accessed on 22 June 2023))
	$X2 \geq FA * (1 - MDRFA) * 15$	2. “Regulations on the Protection and Management of Forests in Guangdong Province” (https://www.gd.gov.cn/zwgk/wjk/zcfgk/content/post_2523665.html (accessed on 22 June 2023))
Grassland area	$X3 \geq GA * (1 - MDRGA) * 15$	Estimation based on historical dataset
Unused land area	$X3 \leq 1.5 * GA$ $X6 \geq ULA * (1 + MIRULA)$	
Water area	$X4 = WA$	1. “Guangzhou Water Management Regulations” (https://www.gd.gov.cn/zwgk/wjk/zcfgk/content/post_2531887.html (accessed on 22 June 2023))
		2. “Measures for the Administration of Guangzhou Municipal Construction Projects Occupying Waters” (https://www.gd.gov.cn/zwgk/wjk/zcfgk/content/post_2531521.html (accessed on 22 June 2023))
Ecological land Construction land area	$X2 + X3 + X4 \geq RLEP$	1. “Guangzhou City Territorial Spatial Master Plan (2018–2035)” (http://ghzyj.gz.gov.cn/zwgk/ztzl/gtkjgh/gzxx/content/post_6484475.html (accessed on 22 June 2023))
	$X5 \leq UDB$ $X5 > CLA$	2. “Outline of the Fourteenth Five-Year Plan for the National Economic and Social Development of Guangzhou Municipality and the Vision 2035” (https://www.gz.gov.cn/zwgk/fggw/szfwj/content/post_7288094.html (accessed on 22 June 2023))
Economic development goals	$\sum X_i * E_i \geq EE * (1 + \text{increase rate}) * 15$	
Development intensity	$X5 / TA < 0.3$	

Notes: E_i denotes the economic coefficient of land use type i ; TA denotes total area; CLQ denotes cultivated land quantity; BPCLA denotes basic permanent cultivated land area; LCS denotes low-carbon-oriented scenario; FA denotes forest area; MDRFA denotes maximum decrease rate of forest area in past decade; GA denotes grassland area; MDRGA denotes maximum decrease rate of grass land area in past decade; ULA denotes unused land area; MIRULA denotes maximum increase rate of unused land area in past decade; WA denotes water area; RLEP denotes red line for ecological protection; UDB denotes urban development boundary; CLA denotes construction land area; EE denotes economic efficiency; IR denotes increase rate.

2.2.3. Spatial Simulation of Land Use Based on Optimized CA Method

In our study, the probability of land use was predicted using the CNN–RF model. CNN was coupled with the RF classifier to determine the nonlinear relationship between numerous factors and land use types, which can be used to calculate the probability of

different land types for each pixel. Land use change data and factor data were included in the input data of the CNN–RF model. Land use data in 2015 and 2020 were used to explore the land use change, which was encoded into seven categories: 0, 1, 2, 3, 4, 5, and 6. Code 0 denotes unchanged, and codes 1, 2, 3, 4, 5, and 6 indicate the six types of cultivated land, forest, grass land, water, construction land, and unused land, respectively, that have been converted from other land use types. Then, land use change data were divided into small patches from which the sample can be chosen randomly as the label data of model input. There are many factors of the change in land use, such as the digital elevation model data, the slope and aspect included in the physical geography data, and the gross domestic product, population density and points of interest included in the socioeconomic data. Factor raster data were divided into small patches, the same as the land use change data, according to their corresponding spatial relationship, and were stacked into different bands in a raster layer.

The framework of the CNN–RF model is shown in Table 4. Part of CNN, the Python library Shapely, and GDAL were used to read the raster dataset and convert the data into digital information. Through the library Shapely, land use change data were divided into small land patches according to the ground truth whose centroid could be extracted. Then, windows with a size of 50×50 were constructed around the row–column positions of centroids, and the factor raster layer and land use were divided into small regular patches. Thirty factor layers were used to predict the probability for each pixel in this paper, resulting in a 3D matrix size of $30 \times 50 \times 50$ for each random sample.

Table 4. Structure of the CNN–RF model.

Order	Layer Name	Input Size	Kernel Size	Output Size
1	Convolution layer	$30 \times 50 \times 50$	3×3	$16 \times 48 \times 48$
2	Max-pooling	$16 \times 48 \times 48$	2×2	$32 \times 24 \times 24$
3	Convolution layer	$32 \times 24 \times 24$	3×3	$32 \times 22 \times 22$
4	Max-pooling	$32 \times 22 \times 22$	2×2	$32 \times 11 \times 11$
5	Convolution layer	$32 \times 11 \times 11$	3×3	$32 \times 9 \times 9$
6	Fully connection	1×2592	Null	1×96
7	SoftMax	1×96	Null	1×6

Notes: The SoftMax layer will be replaced by a random forest classifier in the following study.

The high-level features of the factors were extracted by CNN, which can be used in RF to classify the land. The seven network layers in the CNN structure are as follows: two pooling layers, three convolution layers, one fully connected layer, and a SoftMax classifier layer. The first layer is a convolution layer with a 3×3 convolution kernel, and a $16 \times 48 \times 48$ feature map is output. The second layer is the 2×2 max-pooling layer that can export a $32 \times 24 \times 24$ feature map. The third layer is a convolution layer with a 3×3 convolution kernel, and a $32 \times 22 \times 22$ feature map is obtained. The fourth layer is also the 2×2 max-pooling layer, producing a $32 \times 11 \times 11$ feature map. The fifth layer is also a convolution layer, like the first layer, yielding a $32 \times 9 \times 9$ feature map. The sixth layer is a fully connected layer by which the 2692 features were reduced to 96 features. The seventh layer is a SoftMax layer whereby the probability of various land use types can be calculated. The type with the highest probability is the predicted type.

However, the performance of RF is better than that of the SoftMax classifier. Thus, the SoftMax classifier is replaced by RF in this paper to discover the relationship between the high-level features extracted by layers before the SoftMax classifier and land use types. Previous studies showed that RF is the most effective classifier and can perform better than other classifiers [47]. RF is integrated by many decision trees; the result of RF may be the average value or the plurality of all the results from the decision trees, which can improve predictive accuracy and control overfitting [48]. In this paper, a CNN model with high accuracy needs to be trained. Then, RF is used to replace the SoftMax classifier and train

the RF using the high-level features extracted by the CNN. Finally, the CNN–RF model is used to predict the probability of various land use types.

Artificial neural networks (ANNs) were used to predict the probability of various land use types in previous studies. Although ANNs performed well in former studies, the ANNs only focus on the relationship between land use types and factors on an independent grid. The land use type on an independent grid is influenced not only by the factors on this grid but also the factors of the grid neighborhood, which can be considered more comprehensively by the CNN–RF model.

Then the spatial pattern of land use is simulated using CA method. The multiple CA model is used to simulate the future spatial pattern of land use. After predicting the probabilities of various land use types and obtaining the demands determined by the Linear Programming model, the probability layers are used as the input of the multiple CA model to simulate the future spatial pattern of land use. The self-adaptive inertia and competition mechanism CA of the FLUS model are used as the CA module in the paper [30]. CA consists of three elements, namely, cellular status, transformation rules, and neighborhood cellular, in which the transfer rules are the most important in the changing of cellular status. Aside from the probability predicted by the CNN–RF model, the neighborhood effects, inertia coefficients, and conversion cost were also included in the combined probability of the cellular in the FLUS model. The neighborhood effects are similar to the traditional CA; for a specific grid cell p , the neighborhood effects of land use i are defined via the following formula:

$$\Omega_{p,k}^t = \frac{\sum_{N \times N} \text{con}(c_p^{t-1} = k)}{N \times N - 1} \times w_i \quad (4)$$

where the $\sum_{N \times N} \text{con}(c_p^{t-1} = i)$ denotes the total number of grid cells covered by land use k after the last iteration time $t - 1$ in the $N \times N$ window. Because the different land use types have dissimilar neighborhood effects, w_i is the neighborhood weight for land use i obtained by experts' experiential knowledge or the results of multiple tests.

Inertia coefficients can describe the competition and interaction between different land use types during the CA iterations. The inertia coefficients of various land use types can be adapted according to the difference between land use demands and the number of ground truth grids for land use types, as follows:

$$Inertia_i^t = \begin{cases} Inertia_i^{t-1} & \text{if } |D_i^{t-1}| \leq |D_i^{t-2}| \\ Inertia_i^{t-1} \times \frac{D_i^{t-2}}{D_i^{t-1}} & \text{if } D_i^{t-1} < D_i^{t-2} < 0 \\ Inertia_i^{t-1} \times \frac{D_i^{t-1}}{D_i^{t-2}} & \text{if } 0 < D_i^{t-2} < D_i^{t-1} \end{cases} \quad (5)$$

where $Inertia_i^t$ denotes the inertia coefficient at iteration time t of land use type i ; D_i^{t-1} is the difference between the demand of land use i and the grid count covered by land use i .

Conversion cost indicates the difficulty of converting land use type i to other land use types. The value of conversion cost ranges from 0 to 1, and the closer it is to 1, the more difficult it is to convert.

The combined probability of a specific cellular grid is defined as follows:

$$TP_{p,j}^t = P_{p,j} \times \Omega_{p,j}^t \times Inertia_j^t \times (1 - C_{i \rightarrow j}) \quad (6)$$

where $TP_{p,j}^t$ is the combined probability of grid cell p converting from the land use type i at iteration time $t - 1$ to land use type j at iteration time t ; $P_{p,j}$ denotes the probability of cell p being covered by land use type j ; $\Omega_{p,j}^t$ denotes the neighborhood effect of land use j on grid cell p at iteration time t ; $Inertia_j^t$ is the inertia coefficient of land use type j at iteration time t , and $C_{i \rightarrow j}$ denotes the conversion cost from land use type i to the target land use type j .

3. Results

3.1. Spatial and Temporal Changes of Land Use and Carbon Emissions

3.1.1. Changes of Land Use Structure

Table 5 illustrates the change in the proportion of land use types between 2010 and 2020. Forest makes up the largest proportion of land at 44.21% in 2010, but this slightly decreases by 0.59% from 2010 to 2020. Cultivated land proportion ranks second and exhibits the same slight decreasing trend from 31.82% to 30.99%. The substantial encroachment by other land types during the change results in the largest reduction for water from 7.38% to 5.69%. Except for unused land, construction land is the only land use type that increases from 16.41% to 19.64%. The expansion of construction land is always accompanied by the encroachment of other land types, which causes damage to the ecological environment and increases the difficulty of controlling carbon emissions.

Table 5. Historical quantity of land use change (/km²).

Land Use Type	2010	Percentage	2015	Percentage	2020	Percentage
Cultivated land	2366	31.82%	2264	30.45%	2304	30.99%
Forest	3287	44.21%	3333	44.83%	3243	43.62%
Grassland	12	0.16%	6	0.08%	3	0.04%
Water	549	7.38%	495	6.66%	423	5.69%
Construction land	1220	16.41%	1336	17.97%	1460	19.64%
Unused land	1	0.01%	1	0.01%	2	0.03%

Table 6 shows the transfer areas and land use change types for each land use type. Figure 3 reveals the spatial distribution of land use change types. Cultivated land transfers most actively during land use change. The conversion of other land use types to cultivated land and construction land is distributed broadly in Guangzhou. Forest of 210 km² was converted into cultivated land located in central and northern Guangzhou. Moreover, 118 km² of water converted into cultivated land is concentrated in southern Guangzhou, especially in Nansha District. Due to the influence of the policy of “returning farmland to forests”, cultivated land of 173 km² was transferred to forest, which was scattered in the central area of Guangzhou. Aside from unused land, only 3.7026 km² of construction land was turned into other land use types, which is the lowest figure among the various land use types. The largest part of inflow for construction land was cultivated land, at 208 km², centered on Huadu and Baiyun Districts, and spreading in all directions. Despite the implementation of the policy of “returning farmland to forests” and the Management Measures for The Occupation of Waters by Construction Projects in Guangzhou, the ecological land use types of forest, water, and grassland were transformed to cultivated land and construction land with the rapid development of socioeconomic and urban expansion.

Table 6. Land use transfer matrix (km²).

2020 2010	Cultivated Land	Forest	Grassland	Water	Construction Land	Unused Land
Cultivated land	1971	173	2	12	208	0.1377
Forest	210	3067	0.3537	0.2025	10	0
Grass land	4	0.468	1	0.1089	5	0.5382
Water	118	2	0.1458	407	22	0.4599
Construction land	0.3618	0.0297	0	3	1216	0.0009
Unused land	0.0378	0.0036	0.0153	0	0.3249	0.4383

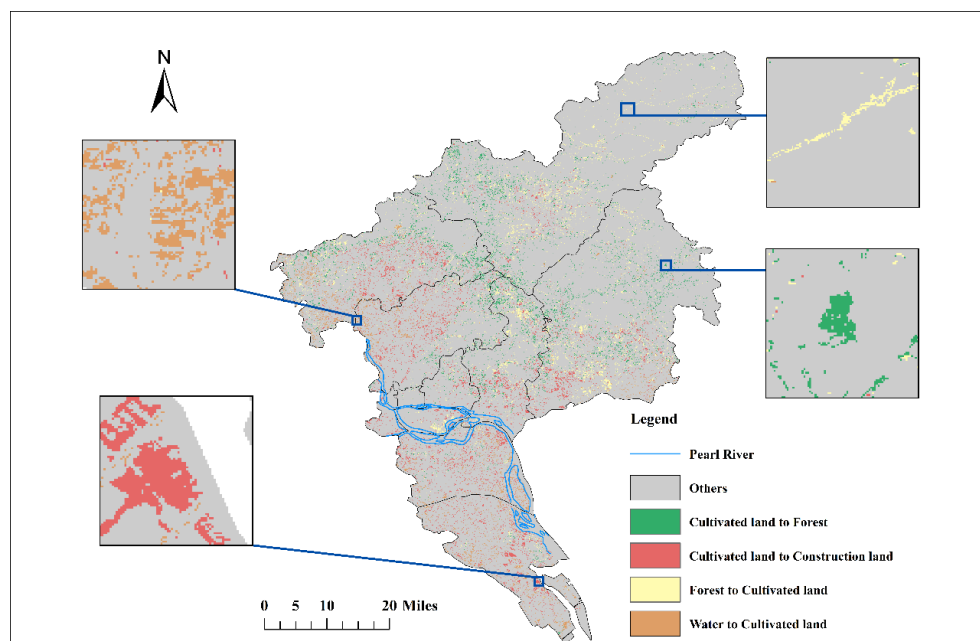


Figure 3. Land use change types and spatial distribution.

3.1.2. Changes of Carbon Emissions in Guangzhou

Figure 4 shows the changes in average carbon emissions at the village level. The carbon emissions of Guangzhou show an overall downward trend from 2005 to 2020. With the industrial transformation and upgrading, as well as the energy structure adjustments, in Guangzhou, the carbon emissions of Guangzhou dropped from 6,641,000 tons in 2005 to 5,288,000 tons in 2020. According to the requirements of the “Guangzhou Carbon Peak Implementation Program”, before 2030, Guangzhou’s carbon emissions need to continue to maintain a downward trend, and a path to increase sinks and reduce emissions is worth exploring. Figure 4 shows that this paper accounts for the carbon emissions per unit of each village in Guangzhou in 2010 and 2020, and classifies them into five categories according to the natural break method. The areas with high carbon emissions gradually spread around the city center in all directions as Guangzhou develops. Carbon emissions in the northern part of Guangzhou are kept low due to the large forest areas. The considerable reduction in carbon emissions in the central city is caused by the evident decrease in the carbon emission coefficient of construction land with the implementation of a series of low-carbon policies.

3.2. Prediction of Land Use Structure in Multiple Scenarios

The land use structure and carbon emissions of Guangzhou under multiple scenarios in 2035 are shown in Tables 7 and 8. The quantities of the six land use types under different scenarios in 2035 meet the quantitative requirements in the existing planning documents, or are consistent with the changes in the land category areas in the historical years.

Under the natural development scenario, the total carbon emissions of Guangzhou will reach 51,458,000 tons in 2035, which is 2.32% lower than in 2020. In terms of land use structure, water has shown the largest decline of 37.75%. The areas of grassland and forest, land types with carbon sink capacity, decrease by 36.27% and 7.48%, respectively. The area of construction land increases by 25.27% from 2020. However, the carbon emission from construction land under the natural development scenario in 2035 decreases by 2.54% with the development of carbon emission-controlling technology.

Under the low-carbon-oriented scenario, the total carbon emissions decline by 18.95% from 2020, which is the largest decline of the three scenarios. This scenario shows a remarkable reduction in carbon emissions while meeting the economic growth rate target. Forest and grassland, which are carbon sinks, rise by 0.10% and 50.11%, respectively.

The area of construction land does not show a substantial increase under the restriction, increasing by 3.93% compared with 2020, and the total carbon emissions from construction land in 2035 decrease by 19.15% compared with 2020.

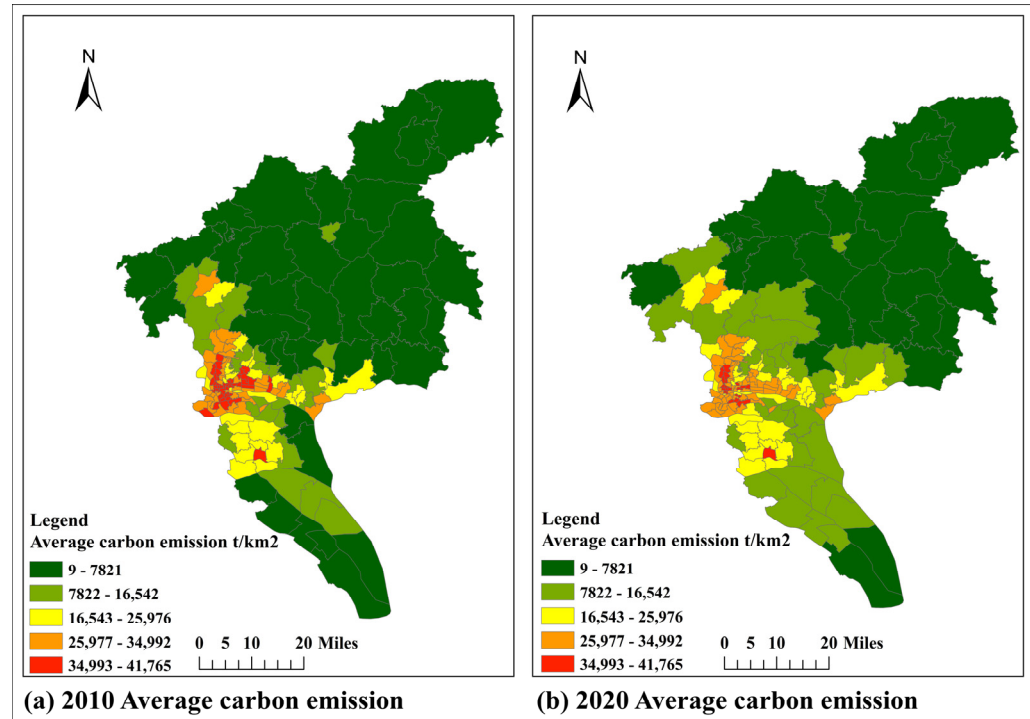


Figure 4. Changes of carbon emissions per unit of each village from 2010–2020.

Table 7. Optimization of land use structure in Guangzhou under different scenarios.

Land Use Types	2020	Natural Development Scenario/km ²	Change Rate	Low-Carbon-Oriented Scenario/km ²	Change Rate	Economic Priority Scenario/km ²	Change Rate
Cultivated land	2304	2338	1.48%	2241	−2.71%	2241	−2.71%
Forest	3243	3000	−7.48%	3246	0.10%	2922	−9.88%
Grassland	3	2	−36.27%	5	50.11%	2	−27.51%
Water	423	263	−37.75%	423	0	423	0
Construction land	1460	1829	25.27%	1518	3.93%	1844	26.28%
Unused land	2	2	−4.13%	2	4.76%	2	4.76%
Total area	7434	7434	0	7434	0	7434	0

Table 8. Change of carbon emissions from land use in Guangzhou under different scenarios.

Land Use Types	2020	Natural Development Scenario/10 ³ t	Change Rate	Low-Carbon-Oriented Scenario/10 ³ t	Change Rate	Economic Priority Scenario/10 ³ t	Change Rate
Cultivated land	330	425	28.77%	407	23.44%	407	23.44%
Forest	−187	−173	−7.48%	−188	0.10%	−169	−9.88%
Grassland	−0.0070	−0.0044	−36.27%	−0.0104	50.11%	−0.0050	−27.51%
Water	−11	−7	−37.75%	−11	0	−11	0
Construction land	52,550	51,213	−2.54%	42,488	−19.15%	51,626	−1.76%
Unused land	−0.0008	−0.0008	−4.13%	−0.0008	4.76%	−0.0008	4.76%
Total	52,682	51,458	−2.32%	42,697	−18.95%	51,854	−1.57%

Under the economic priority scenario, total carbon emissions decrease by 1.57% from 2020, with the lowest decrease compared with the two remaining scenarios. Construction land increases by 26.28% compared with 2020. Due to the orientation of economic

efficiency priority, more cultivated land, forest, and grassland will be converted into construction land and decrease by 2.71%, 9.88%, and 27.51%, respectively.

3.3. Simulated Spatial Pattern of Land Use in 2035

3.3.1. Performance Comparison of ANN-CA Model and CNN-RF-CA Model

The land use change data from 2010 to 2015 and the driving factors in 2015 were used to predict the land use spatial pattern in 2020. The kappa coefficient and overall accuracy were used to assess the performance of the ANN-CA model and the CNN-RF-CA model, respectively. The overall accuracy and kappa coefficient of the CNN-RF-CA model are better than those of the ANN-CA model. More specifically, the kappa coefficient is 0.85 in ANN-CA and 0.89 in CNN-RF-CA, which means the classification effect of CNN-RF-CA is higher than that of ANN-CA. In addition, the overall accuracy of the two models is 0.90 in ANN-CA and 0.93 in CNN-RF-CA, which means the total number of pixels correctly predicted by the CNN-RF-CA model is more than that of the ANN-CA model.

Differences were also observed in the predictive effectiveness of the two models in different regions. Three classic places, namely, the central part of Conghua District, the northern part of Huadu District, and the southern part of Nansha District, were selected to compare the effectiveness of spatial prediction (Figure 5). In the central part of Conghua District, the simulated result of the ANN-CA model is different from in other images, in which forest is encroached upon by construction land. The output of CNN-RF-CA is more similar to the ground conditions, which means CNN-RF-CA performs better than ANN-CA in modeling forest and built-up land. In the northern part of Huadu District, part of the Pearl River is encroached upon by construction sites in the output of ANN-CA; however, according to the ground condition, this area should be water, which is more similar to the result of CNN-RF-CA. In the southern part of Nansha District, according to the ground truth, the circled area in Figure 5 should be construction land. The CNN-RF-CA model's simulation results are biased in this area.

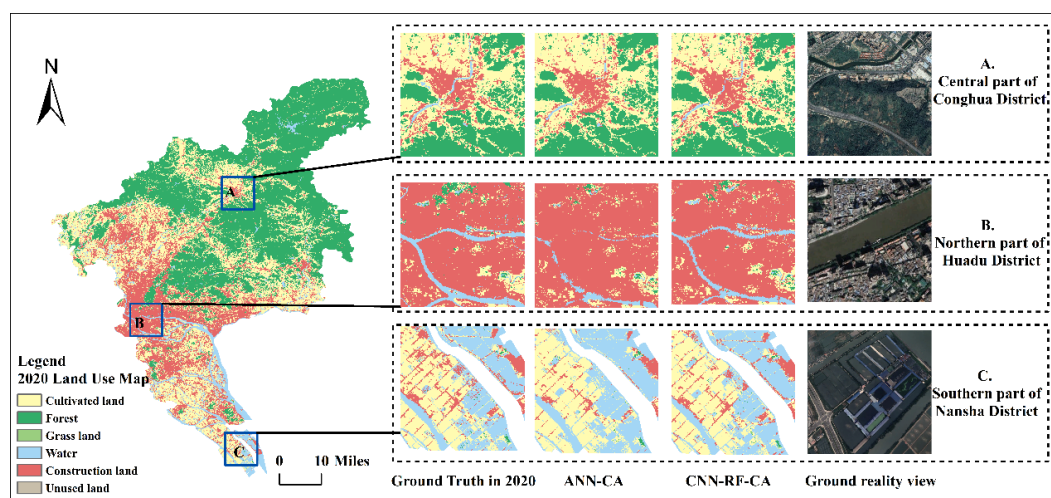


Figure 5. Local comparison of ANN-CA and CNN-RF-CA's simulation results.

The above analysis proves that the performance of the CNN-RF-CA model is better than that of the ANN-CA model. Therefore, the CNN-RF-CA model was used to simulate the spatial pattern in 2035 under multiple scenarios in this paper.

3.3.2. Simulation Results

Figure 6 shows the simulation results of land use pattern in 2035 among different scenarios based on the CNN-RF-CA model. The land use structure under the natural development scenario is set to follow its natural development pattern, with a rapid increase in the construction land under the natural development scenario, and the gradual expansion

from the central city to surroundings area. At the same time, nature reserves are being encroached upon, and forests will be taken over by construction land. Water areas in the west of Guangzhou are to be occupied by construction land. Especially in the southern Baiyun and Yuexiu Districts, most areas of the Baiyun Mountain and Pearl River will be occupied by construction land.

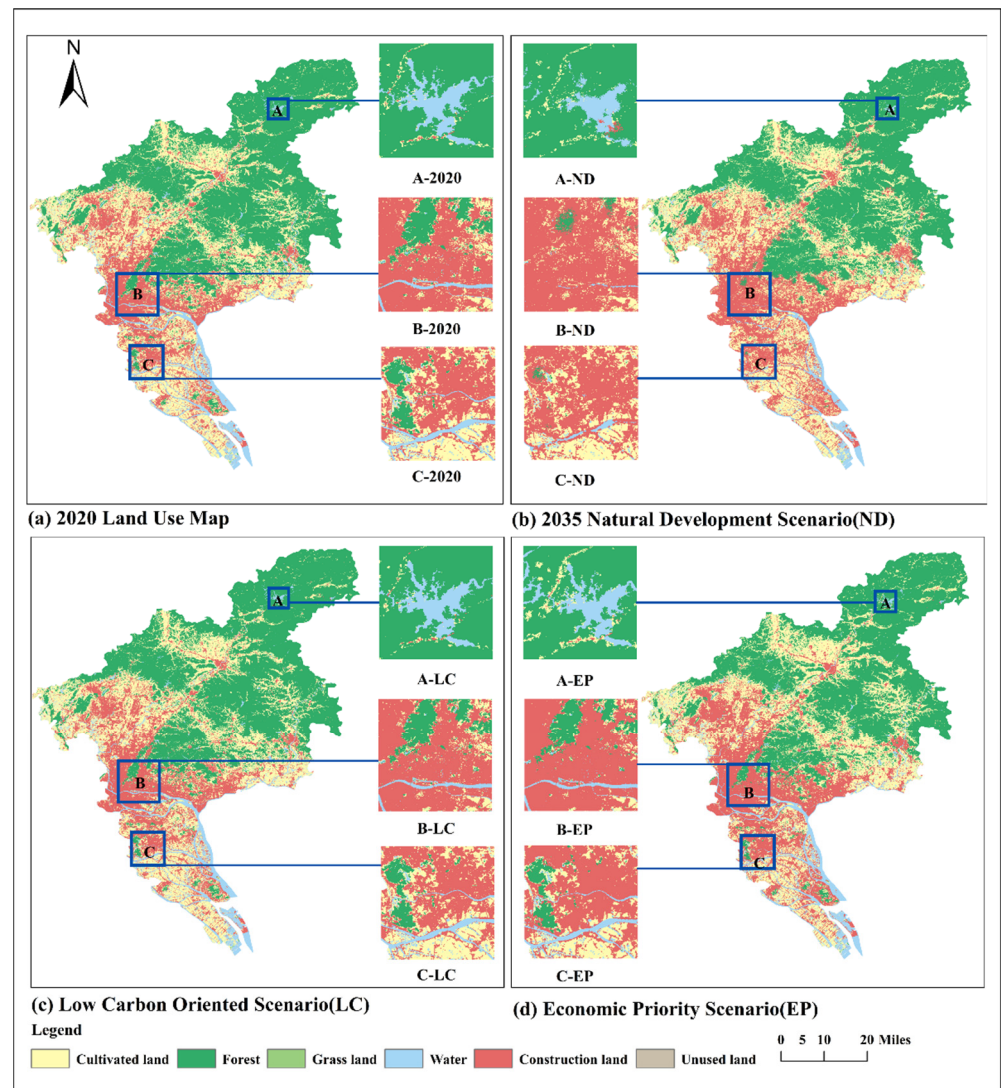


Figure 6. Optimized spatial pattern under different scenarios. A, B, and C represent northern Conghua District, southern Baiyun and Yuexiu District, and western Panyu District, respectively; ND, LC, and EP denote the natural development scenario, the low-carbon-oriented scenario, and the economic priority scenario, respectively.

The substantial expansion of construction land is limited in the scenario of low-carbon orientation. Construction land will expand around the original urban area, which is smaller than in other scenarios. A minor increase in forest is noted. Fragmented cultivated land will be converted into forest, such as the areas surrounding Liuxi Lake in the northern Conghua District.

In the economic priority scenario, construction land will expand remarkably, and its density will increase. Other land types interspersed with construction land will be converted into construction land after 2020. Many cultivated lands and forests will turn into construction land compared with the other scenarios, especially in the central city of Guangzhou. Compared with the natural development scenario, the red line of ecological

protection in Panyu and Nansha Districts is not to be encroached upon, and the ecological protection zones will be preserved.

Comparing the results of optimizing the land use structure and spatial layout under different scenarios reveals that the simulation results of the three future scenarios show the effects of different development strategies on the spatial layout of the land use in Guangzhou. Due to technological progress and the adjustment of the energy structure, the per unit carbon emissions of construction land will be limited, so the total carbon emissions of the three scenarios are reduced compared with that of 2020. In the low-carbon-oriented scenario, the expansion of construction land is inhibited, such as in the northern Huadu District. In the northeastern Conghua District, the forest intensity under the low-carbon-oriented scenario is higher than in other scenarios. In the economic priority scenario and the natural development scenario, the construction land use will still increase. More ecological land in the areas of Baiyun Mountain and Pearl River will be encroached upon under the natural development scenario than in the economic priority scenario. Both the natural development scenario and the low-carbon-oriented scenario show carbon reductions; however, there are great differences with respect to the land use pattern in these two scenarios. An example is that the building density in the central city under the economic priority scenario is higher than that in the low-carbon-oriented scenario, and the forest density in Conghua District under the economic priority scenario is less than that under the low-carbon-oriented scenario.

4. Discussion

China still faces tremendous pressure and challenges in achieving the “dual carbon” goal. Although scholars have conducted substantial research on land use changes in the context of carbon mitigation, there is an urgent need to explore how to achieve the “dual carbon” goal through the optimization of land use patterns to support the low-carbon transformation of the urban development with adequate local studies and experiments. There are two contributions made by this study, which are the integration of pragmatic urban planning in Guangzhou in the process of the prediction of land use, and the embracing of socioeconomic factors in the process of land spatial simulation. At present, the traditional studies on land use and carbon emission primarily apply “ecological–economic” benefit trade-offs to optimize the land use spatial pattern and then evaluate the carbon emissions. This solution undoubtedly ignores the importance of the pre-integration of carbon mitigation into land use planning, as well as the technical prediction and simulation processes [49,50]. In this paper, considering land spatial planning for the city, predictions of land use structure are formed considering carbon reduction goals, and the simulation of low-carbon land use patterns is realized with the adjusted CA models. The simulation results reveal that land use patterns and carbon emissions in different scenarios show great discrepancies, and the low-carbon-oriented scenario demonstrates considerable carbon reduction benefits compared with the natural and economic-oriented scenarios. Intuitively, bottom-up land conversion is driven by the land market, and construction land is the land use type with the highest probability of increasing, which has been justified in a number of extant studies [14,29]. However, with food security and ecological security as the bottom lines in land spatial planning in China, the spatial distributions of cropland and ecological land are necessarily conserved and protected. The top-down control of land use management attempts to balance and synthesize the ecological and socioeconomic benefits. Our study embeds the needs and constraints within land spatial planning into the spatial optimization of land use patterns, which makes low-carbon city development pragmatic.

Technically, the critical procedures involved in calculations or spatial simulation are adjusted and optimized based on empirical studies as well as local situations. First, carbon emission coefficients are determined through the combination of the historical carbon emission data and land use data, as well as extant experiments in Guangzhou. This approach makes carbon emission accounting and linear programming model construction more in line with local characteristics, allowing us to improve the reliability of the model. Second,

the data are integrated into land spatial planning to optimize the results. For instance, in the low-carbon-oriented scenario, the construction land area is 1517.76 km², which conforms to the requirement of the urban development boundary of Guangzhou in 2035. Finally, the simulation uses CNN to generate conversion probabilities, and socioeconomic factors in the research area are integrated during the generation. The simulation accuracy using the Kappa index increases from 0.90 to 0.93, indicating the superiority of the model considering anthropogenic activities. Compared with other similar studies in Guangzhou, the accuracy of the optimized model in this study has been significantly improved [51,52].

In summary, this study focuses on the optimization of the land use pattern in the context of carbon mitigation using the linear programming method and a series of geospatial technologies. It provides theoretical and technical references for green sustainable development and land management, and to achieve synergy between low-carbon transformation and socioeconomic development. In future research, the differentiated demand of land types due to diverse local policies and the regional spatial interaction will be integrated to achieve more accurate and pragmatic planning guidance. Due to the limitations of the experimental dataset, this paper only estimates the carbon emission per unit of each land category based on empirical studies, and does not consider the internal variability of carbon emission intensity within a land category due to population, industry, and tree species. In subsequent studies, carbon emission estimations can be adjusted by combining field experiments, questionnaires, and extant studies to optimize land use robustly in the context of climate change.

5. Conclusions

In this paper, land use pattern is simulated and optimized with the integration of the linear programming model, the Markov Chain model, and the adjusted CA model in different scenarios to realize low-carbon city development, taking Guangzhou as the case study area. The carbon emission coefficient of construction land will decrease from 66,055.34 t/km² to 27,993.95 t/km² annually from 2005 to 2035, whereas the carbon emission coefficient of cultivated land will increase from 84 t/km² to 181 t/km². Lands with a carbon sink function, such as forest land, grassland, water, and unused land, are stable with respect to areas and related carbon mitigation capabilities. In the natural development scenario, cultivated land area and construction land area increase. The low-carbon-oriented scenario shows an increase in forest area and grassland area and a slight rise in the area of construction land and unused land. The expansion of construction land is revealed in the economic priority scenario. In the low-carbon-oriented scenario, the expansion of construction land is effectively controlled, and the density and land use efficiency of construction land are improved. Forest land and grassland show an upward trend, which ensures the normal development of the economy and minimizes carbon emissions. Technically, considering the influence of neighborhood factors for each pixel in the simulation of land use spatial layout, the CNN-RF-CA model performs better than ANN-CA in the simulation. In the future, the spatial land use pattern can be realized through robust models with the integration of land spatial planning, as well as anthropogenic activities, to make spatial optimization more accurate and pragmatic.

Author Contributions: Conceptualization, S.L., M.C. and C.Z.; data curation, S.D., H.L. and Y.Z.; formal analysis, S.L., M.C. and T.L.; methodology, S.L., M.C. and C.Z.; project administration, S.D., H.L., Y.Z. and C.Z.; resources, S.D., H.L., Y.Z. and C.Z.; software, S.L. and M.C.; supervision, S.D., H.L., Y.Z. and C.Z.; writing—original draft, S.L. and M.C.; writing—review and editing, T.L. and C.Z. All authors have read and agreed to the published version of the manuscript.

Funding: This research was funded by the National Natural Science Foundation of China, grant number 41771563; Funds for International Cooperation and Exchange of the National Natural Science Foundation of China, grant number 42211530079; the Fundamental Research Funds for the Central Universities, grant number 2662021JC003; Guangzhou Collaborative Innovation Center of Natural Resources Planning and Marine Technology, grant number 2023B04J0301, 2023B04J0046; Key-Area Research and Development Program of Guangdong Province, grant number 2020B0101130009;

Guangdong Enterprise Key Laboratory for Urban Sensing, Monitoring and Early Warning, grant number No.2020B121202019.

Data Availability Statement: The data presented in this study are available on request from the author.

Conflicts of Interest: The authors declare no conflict of interest.

References

1. Berrang-Ford, L.; Biesbroek, R.; Ford, J.D.; Lesnikowski, A.; Tanabe, A.; Wang, F.M.; Chen, C.; Hsu, A.; Hellmann, J.J.; Pringle, P.; et al. Tracking global climate change adaptation among governments. *Nat. Clim. Chang.* **2019**, *9*, 440–449. [[CrossRef](#)]
2. IPCC. Summary for Policymakers. In *Special Report on Climate Change and Land*; Shukla, P.R., Ed.; WMO: Geneva, Switzerland, 2019.
3. Zhao, R.Q.; Huang, X.J.; Yun, W.J.; Wu, K.N.; Chen, Y.R.; Wang, S.J.; Lu, H.L.; Fang, K.; Li, Y. Key issues in natural resource management under carbon emission peak and carbon neutrality targets. *J. Nat. Resour.* **2022**, *37*, 1123. [[CrossRef](#)]
4. Lal, R. Soil carbon dynamics in cropland and rangeland. *Environ. Pollut.* **2002**, *116*, 353–362. [[CrossRef](#)] [[PubMed](#)]
5. Huang, X.J.; Zhang, A.L.; Zhao, R.Q.; Gao, F.; Zhang, H.H. Carbon Emission Peak, Carbon Neutrality and Territorial Spatial Planning Implementation Mechanism. *Mod. Urban Res.* **2022**, *1*, 1–5. [[CrossRef](#)]
6. Yi, D.; OU, M.; Guo, J.; Han, Y.; Yi, J.L.; Ding, G.Q.; Wu, W.J. Progress and prospect of research on land use carbon emissions and low-carbon optimization. *Resour. Sci.* **2022**, *44*, 1545–1559. [[CrossRef](#)]
7. Huang, X.J.; Zhang, X.Y.; Lu, X.H.; Wang, P.Y.; Qin, J.Y.; Jiang, Y.C.; Liu, Z.M.; Wang, Z.; Zhu, A.X. Land development and utilization for carbon neutralization. *J. Nat. Resour.* **2021**, *36*, 2995–3006. [[CrossRef](#)]
8. Zhang, M.; Gan, C.L.; Chen, Y.R.; Chen, L. Carbon emission efficiency and optimization of low carbon for construction land development intensity in China according to provincial panel data. *Resour. Sci.* **2016**, *38*, 265–275. [[CrossRef](#)]
9. Dangwal, B.; Rana, S.K.; Negi, V.S.; Bhatt, I.D. Forest restoration enhances plant diversity and carbon stock in the sub-tropical forests of western Himalaya. *Trees For. People* **2022**, *7*, 100201. [[CrossRef](#)]
10. Zhang, C.Y.; Zhao, L.; Zhang, H.; Chen, M.N.; Fang, R.Y.; Yao, Y.; Zhang, Q.P.; Wang, Q. Spatial-temporal characteristics of carbon emissions from land use change in Yellow River Delta region, China. *Ecol. Indic.* **2022**, *136*, 108623. [[CrossRef](#)]
11. Zhong, S.C.; Wang, W.Z.; Yan, C.L. Research on the response of spatial allocation of urban construction land in China's provinces under the goal of carbon emission reduction. *J. Nat. Resour.* **2023**, *38*, 1896–1918. [[CrossRef](#)]
12. Chen, K.X.; Tao, W.H.; Fang, X.L.; Wei, J.M. Carbon Neutrality Assessment and Planning Application Path in Territorial Spatial Planning. *Planners* **2022**, *38*, 134–141. [[CrossRef](#)]
13. Ding, M.L.; Yang, X.N.; Zhao, R.Q.; Zhang, Z.P.; Xiao, L.G.; Xie, Z.X. Optimization of territorial space pattern under the goal of carbon neutrality: Theoretical framework and practical strategy. *J. Nat. Resour.* **2022**, *37*, 1137–1147. [[CrossRef](#)]
14. Huang, S.; Xi, F.; Chen, Y.; Gao, M.; Pan, X.; Ren, C. Land Use Optimization and Simulation of Low-Carbon-Oriented—A Case Study of Jinhua, China. *Land* **2021**, *10*, 1020. [[CrossRef](#)]
15. Zhu, E.; Deng, J.; Zhou, M.; Gan, M.; Jiang, R.; Wang, K.; Shahtahmasebi, A. Carbon emissions induced by land-use and land-cover change from 1970 to 2010 in Zhejiang, China. *Sci. Total Environ.* **2019**, *646*, 930–939. [[CrossRef](#)]
16. Ke, Y.H.; Xia, L.L.; Huang, Y.S.; Li, S.E.; Zhang, Y.; Liang, S.; Yang, Z.F. The carbon emissions related to the land-use changes from 2000 to 2015 in Shenzhen, China: Implication for exploring low-carbon development in megacities. *J. Environ. Manag.* **2022**, *319*, 115660. [[CrossRef](#)] [[PubMed](#)]
17. Fryer, J.; Williams, I.D. Regional carbon stock assessment and the potential effects of land cover change. *Sci. Total Environ.* **2021**, *775*, 145815. [[CrossRef](#)]
18. Wang, G.; Han, Q.; De Vries, B. The multi-objective spatial optimization of urban land use based on low-carbon city planning. *Ecol. Indic.* **2021**, *125*, 107540. [[CrossRef](#)]
19. Woodwell, G.M.; Hobbie, J.E.; Houghton, R.A.; Melillo, J.M.; Peterson, B.J.; Shaver, G.R. Global Deforestation: Contribution to Atmospheric Carbon Dioxide. *Sci. New Ser.* **1983**, *222*, 1081–1086. [[CrossRef](#)] [[PubMed](#)]
20. Wu, M.; Ren, L.; Chen, Y.R. Simulation of Urban Land Use Carbon Emission System based on a System Dynamic Model: Take Wuhan as an Example. *China Land Sci.* **2017**, *31*, 29–39. [[CrossRef](#)]
21. Fang, J.Y.; Chen, A.P. Dynamic Forest Biomass Carbon Pools in China and Their Significance. *J. Integr. Plant Biol.* **2001**, *43*, 967–973. [[CrossRef](#)]
22. Fang, J.Y.; Guo, Z.D.; Piao, S.L.; Chen, A.P. Estimation of carbon sinks in terrestrial vegetation in China from 1981 to 2000. *Sci. Sin. Terrae* **2007**, *37*, 804–812. [[CrossRef](#)]
23. Li, J.; Guo, X.; Chuai, X.; Xie, F.J.; Yang, F.; Gao, R.Y.; Ji, X.P. Reexamine China's terrestrial ecosystem carbon balance under land use-type and climate change. *Land Use Policy* **2021**, *102*, 105275. [[CrossRef](#)]
24. Sun, J.W.; Zhao, R.Q.; Huang, X.J.; Chen, Z.G. Research on Carbon Emission Estimation and Factor Decomposition of China from 1995 to 2005. *J. Nat. Resour.* **2010**, *25*, 1284–1295. [[CrossRef](#)]
25. Jia, K.L.; Li, X.Y.; Wei, H.M.; Liu, R.L.; Li, H.Y.; Yang, S.Y. Spatial differentiation and risk of land use carbon emissions in county region of Ningxia. *Arid Land Geogr.* **2023**, *1*–13.
26. Zhou, L.; Dang, X.; Sun, Q.; Wang, S.H. Multi-scenario simulation of urban land change in Shanghai by random forest and CA-Markov model. *Sustain. Cities Soc.* **2020**, *55*, 102045. [[CrossRef](#)]

27. Gao, L.; Tao, F.; Liu, R.; Wang, Z.; Leng, H.; Zhou, T. Multi-scenario simulation and ecological risk analysis of land use based on the PLUS model: A case study of Nanjing. *Sustain. Cities Soc.* **2022**, *85*, 104055. [[CrossRef](#)]
28. Zeng, Y.N.; Wang, H.M. Optimization of land use structure for low-carbon targets in Haidong City, Qinghai Plateau. *Resour. Sci.* **2015**, *37*, 2010–2017.
29. Li, D.C.; Lu, J.Q.; Xie, X.W.; Yu, H.; Li, Y.; Wu, S. Optimization simulation of land space zoning based on the classification constraints of main functional zones from the perspective of carbon neutrality: A case study of Fujian Province. *Acta Ecol. Sin.* **2022**, *42*, 10111–10126. [[CrossRef](#)]
30. Liu, X.; Liang, X.; Li, X.; Xu, X.; Ou, J.; Chen, Y.; Li, S.; Wang, S.; Pei, F. A future land use simulation model (FLUS) for simulating multiple land use scenarios by coupling human and natural effects. *Landsc. Urban Plan.* **2017**, *168*, 94–116. [[CrossRef](#)]
31. Liang, X.; Guan, Q.; Clarke, K.C.; Liu, S.; Wang, B.; Yao, Y. Understanding the drivers of sustainable land expansion using a patch-generating land use simulation (PLUS) model: A case study in Wuhan, China. *Comput. Environ. Urban Syst.* **2021**, *85*, 101569. [[CrossRef](#)]
32. Verburg, P.H.; Soepboer, W.; Veldkamp, A.; Limpiada, R.; Espaldon, V.; Mastura, S.A. Modeling the Spatial Dynamics of Regional Land Use: The CLUE-S Model. *Environ. Manag.* **2002**, *30*, 391–405. [[CrossRef](#)] [[PubMed](#)]
33. Shi, H.X.; Mu, X.M.; Zhang, Y.L.; Lv, M.Q. Study on carbon emission effects of different land use types in Guangyuan City, Sichuan Province. *Soil Water Conserv. Bull.* **2012**, *32*, 101–106. [[CrossRef](#)]
34. Gai, Z.X.; Zhan, W.X.; Wang, H.Y.; Du, G.M. Spatio-temporal Differentiation Characteristics and Formation Mechanism of Carbon Emission from Cultivated Land Use Transformation. *J. Agric. Mach.* **2022**, *53*, 187–196. [[CrossRef](#)]
35. Lai, L. Carbon Emission Effect of Land Use in China. Ph.D. Thesis, Nanjing University, Nanjing, China, 2010.
36. Kuang, Y.Q.; Ouyang, T.P.; Zou, Y.; Liu, Y.; Li, C.; Wang, D.H. Present Situation of Carbon Source and Sink and Potential for Increase of Carbon Sink in Guangdong Province. *China Popul. Resour. Environ.* **2010**, *20*, 56–61. [[CrossRef](#)]
37. Sun, H.; Liang, H.M.; Chang, X.L.; Cui, Q.; Tao, Y. Land Use Patterns on Carbon Emission and Spatial Association in China. *Econ. Geogr.* **2015**, *35*, 154–162. [[CrossRef](#)]
38. Hu, L. Research on the Mechanism of How Urbanization Effect on Carbon Emissions in China. *Clim. Change Res.* **2016**, *12*, 341–347. [[CrossRef](#)]
39. Liu, G.; Zhang, F. How do trade-offs between urban expansion and ecological construction influence CO₂ emissions? New evidence from China. *Ecol. Indic.* **2022**, *141*, 109070. [[CrossRef](#)]
40. Yuan, K.H.; Mei, Y.; Chen, Y.R.; Lan, M.T. Temporal and spatial evolution and influencing mechanism of construction land intensive utilization on carbon emissions efficiency in China. *Resour. Sci.* **2017**, *39*, 1882–1895. [[CrossRef](#)]
41. Lu, M.; Yan, H.C.; Hu, W.X.; Wang, L.; Peng, L. Analyze on the rule of carbon emission of different land use patterns in Guangdong province. *Guangdong Agric. Sci.* **2012**, *39*, 1–5+9. [[CrossRef](#)]
42. Li, B.; Zhang, J.B. Study on Carbon Effects and Spatial Differences Based on Changes in China's Agricultural Land Use. *Econ. Geogr.* **2012**, *32*, 135–140. [[CrossRef](#)]
43. Wang, W.S.; Munkhnasan, L.; Lee, W.K. Land use and land cover change detection and prediction in Bhutan's high-altitude city of Thimphu, using cellular automata and Markov chain. *Environ. Chall.* **2021**, *2*, 100017. [[CrossRef](#)]
44. Chen, C.J.; Liu, Y.H. Spatiotemporal changes of ecosystem services value by incorporating planning policies: A case of the Pearl River Delta, China. *Ecol. Model.* **2021**, *461*, 109777. [[CrossRef](#)]
45. He, H.S.; Zhao, Y.H.; Wu, J.S. Simulation of urban landscape pattern under the Influence of Low Carbon: A Case Study of Shenzhen. *Acta Ecol. Sin.* **2021**, *41*, 8352–8363. [[CrossRef](#)]
46. Cao, S.; Jin, X.B.; Yang, X.H.; Sun, R.; Liu, J.; Han, B.; Xu, W.Y.; Zhou, Y.K. Coupled MOP and GeoSOS-FLUS models research on optimization of land use structure and layout in Jintan district. *J. Nat. Resour.* **2019**, *34*, 1171–1185. [[CrossRef](#)]
47. Fernández-Delgado, M.; Cernadas, E.; Barro, S.; Amorim, D. Do we need hundreds of classifiers to solve real world classification problems? *J. Mach. Learn. Res.* **2014**, *15*, 3133–3181.
48. Biau, G. Analysis of a random forests model. *J. Mach. Learn. Res.* **2012**, *13*, 1063–1095.
49. Tayier, K.; Li, H.; Aierken, G.; Yin, Z.C.; Wu, H. Spatio-temporal Evolution and Prediction of Carbon Emissions in Urumqi Region Based on FLUS and Grey Prediction Model. *J. Soil Water Conserv.* **2023**, *37*, 214–226. [[CrossRef](#)]
50. Zhang, J.X.; Zhang, C.F.; Dong, H.; Zhang, L.W.; He, S.C. Spatial-Temporal Change Analysis and Multi-Scenario Simulation Prediction of Land-Use Carbon Emissions in the Wuhan Urban Agglomeration, China. *Sustainability* **2023**, *15*, 11021. [[CrossRef](#)]
51. Li, W.Q.; Lan, Z.Y.; Chen, D.Q.; Zheng, Z.J. Multi-scenario Simulation of Land Use and its Spatial-temporal Response to Ecological Risk in Guangzhou City. *Bull. Soil Water Conserv.* **2020**, *40*, 204–210. [[CrossRef](#)]
52. Lin, S.L.; Wang, F. Simulation and analysis of land use scenarios in Guangzhou based on the PLUS model and traffic planning scenario. *J. Agric. Resour. Environ.* **2023**, *40*, 557–569. [[CrossRef](#)]

Disclaimer/Publisher's Note: The statements, opinions and data contained in all publications are solely those of the individual author(s) and contributor(s) and not of MDPI and/or the editor(s). MDPI and/or the editor(s) disclaim responsibility for any injury to people or property resulting from any ideas, methods, instructions or products referred to in the content.